Yamagata Med J (ISSN 0288-030X) 2017 ; 35(2) : 21-32
DOI 10.15022/00004195

Analysis of signal transducers using flow cytometry is useful for detection of contractive and fluctuating signals

Yuji Takeda, Hidetoshi Nara, Hironobu Asao

Department of Immunology, Yamagata University Faculty of Medicine
(*Accepted March 1, 2017*)

Abstract

Investigation of signal transduction mechanisms is important for development of therapy and understanding complex life systems. In this study, to establish a novel recognition method of signal transduction pathways, we investigated signal transducers using flow cytometry.

The flow cytometric measurement shows a mean phosphorylation level (mean of fluorescence intensity, MFI) and a deviation of the phosphorylation level (coefficient variation, CV) in a cluster of cells. As a model of signal pathways, Jurkat cells (T cell leukemia cell line) were stimulated with interleukin-21 or interferon-α, and signal transducers and activators of transcription (STATs) and extracellular signal-regulated kinase (ERK) 1/2 were measured using flow cytometry. Furthermore, peripheral blood was stimulated, and then various signal transducers of the lymphocytes and neutrophils were analyzed with MFI and CV.

After the stimulation, the increase of STATs MFI induced a temporal change of CV. On the other hand, the decrease of ERK1/2 phosphorylation accompanied the sustained increase of CV. Finally, we classified the signaling characters into five types using a combination of MFI and CV. These findings contribute to an explanation of the known relationship between signal transducers and stimulants on each cell subset. Therefore, this method may be useful to discover a causal relationship between stimulants and signal transducers in complex systems.

Key words: complex system, flow cytometry, signal transduction

Introduction

Signal transduction pathways are important for understanding homeostatic mechanisms and specific reactions[1)–3)]. Many molecular mechanisms related to signal transduction pathways have been identified and are leading to the development of many useful medicines. Although the schema of these pathways is useful for understanding the specific hierarchical pathways, it is difficult to recognize concurrently activated signals and growing factors in one schema.

Recently, new methodologies, such as various comprehensive analyses (proteome, metabolome, or genome) and computational studies, have been developed to investigate various hyper-complex systems in life sciences[4)–7)]. These analyses identified numerous molecules that help in differentiating samples. However, growing factors identified by these high-dimensional approaches cannot always lead to discovery of a causal relationship in signal transduction pathways. Specifically, a comparison of the average molecular amount in cell lysis samples cannot easily clarify the pathways in heterogeneous cells and asynchronously activated cells[8), 9)]. Furthermore, the pathways are spatio-temporally regulated by feedback mechanisms, protein modification mechanisms, or cell-to-cell communication[7), 10)]. Thus, discovering the direct cause among the growing factors is very difficult.

In this study, we analyzed signal transducers and activators of transcription (STATs) and extracellular signal-regulated kinase (ERK) 1/2 in the Jurkat cell line as a model of cell signaling. STATs are known to be activated in a receptor-specific manner[11]. For example, STAT1 is activated by stimulation from interferon- α (IFN- α)[12, 13], and STAT3 is activated by stimulation from interleukin (IL)-21[14, 15]. ERK1/2 (MAP kinase family) is a known regulator of cellular proliferation[16, 17]. Furthermore, the ERK1/2 pathway is subsequently activated by various stimulations such as lipopolysaccharide and redox status[18, 19].

Phospho-specific flow cytometry for signal networking has several advantages, such as single cell analysis capability, multi-parameter data acquisition, rapid protocols, and the ability to analyze rare cell subsets, compared with traditional biochemical methods[20]. Recently, the analysis methods of flow cytometry have been combined with various comprehensive analyses[21, 22]. However, a percentage of positive cells or a value of mean of fluorescence intensity (MFI) have been used for these flow cytometric analyses. In this study, we postulated a theoretical method of signaling recognition in complex systems and applied the theory to analysis of signal transduction using coefficient variation (CV). We demonstrated the validity of a novel recognition method using flow cytometry and classification of STATs, ERK1/2, etc., as contractive or fluctuating signals. This novel method will allow the use of bioinformatics to discover a causal relationship between stimulants and signal pathways in complex systems.

Materials and Methods

Jurkat cells

Jurkat cells were obtained from the Department of Immunology at Tohoku University School of Medicine (originally gifted from Ajinomoto Co. Ltd, Tokyo) and maintained in RPMI 1640 (Sigma-Aldrich, St. Louis, MO, USA) supplemented with 10% fetal calf serum (Biowest, Nuaillé, France), 50 U/mL penicillin G potassium, and 50 μg/mL streptomycin sulfate at 37°C in 5% CO_2 with high humidity.

Peripheral blood

This study was approved by the Ethics Committee of Yamagata University Faculty of Medicine (approval number, 265). Peripheral blood was collected from healthy volunteers following informed consent and heparinized by 5 U/mL of low molecular weight heparin. The average age of the donors was 49.3 ± 2.6 years (n = 4). Following sample collection, the blood was immediately transferred into 1.5 mL microtubes and used for experiments.

Cell stimulation with cytokines

Cell stimulation was performed as previously reported[23]. Briefly, Jurkat cells (0.7 to 1 x 10^6 cells/mL, 0.5 mL/tube) or whole peripheral blood cells (0.1 mL/tube) were stimulated with IFN- α (Takeda Pharmaceutical Co. Ltd, Osaka, Japan) or IL-21 (Peprotech, Rocky Hill, NJ, USA) for 10 to 90 min in microtubes at 37°C. In several experiments, the cells were preincubated with MEK1/2 inhibitor (U0126, Thermo Fisher Scientific, Waltham, MA, USA) for 10 min at 37°C. After the stimulation, the cells were immediately fixed by Lyse/Fix buffer (BD Biosciences, San Jose, CA, USA) for 10 min at 37°C. The fixed cells were packed by centrifugation at 800 x g for 1 min and then stocked in 90% methanol (0.3 mL/tube) at −20°C until flow cytometric analysis.

Flow cytometric analysis

The fixed cells were washed with 0.8 mL phosphate-buffered saline (PBS) and suspended in PBS containing 1% bovine serum albumin and 0.1% sodium azide. The cells were transferred into V-bottom 96-well plates and were incubated with each antibody for 45 min at 22-25°C. The antibodies used in this study are summarized in Table 1[23]. After the reaction, the cells were washed with PBS and measured by flow cytometry (ec800, Sony, Tokyo, Japan; FACSCanto II, BD Biosciences, Franklin Lakes, NJ, USA). Debris was excluded from the analysis by dim-forward and side-scatter gating. The fluorescence intensity and robust coefficient value (CV) were analyzed using FlowJo software (v6.2, TreeStar, Ashland, OR, USA). The calculation formula for robust CV is as follows: CV = 100 × 1/2 [(Intensity at 84.13 percentile) − (Intensity at 15.87

Table 1. List of antibodies used in this study

Surface antigen	Label	Subclass	Clone	Supplier
CD3	PE	IgG1	UCHT1	BD
CD16	PE	IgG1	3G8	BD
Signal transducer	**Label**	**Subclass**	**Clone**	**Supplier**
STAT1 (pY701)	Alexa488	IgG2a	4a	BD
STAT3 (pY705)	Alexa488	IgG2a	4/P-STAT3	BD
STAT5 (pY694)	Alexa488	IgG1	47/Stat5	BD
ERK1/2 (pT202/pY204)	Alexa647	IgG1	20A	BD
Akt (pS473)	V450	IgG1	M89-61	BD
p38MAPK (pT180/pY182)	Alexa488	IgG1	36/p38	BD
NF-kBp65 (pS536)	Alexa647	Rabbit IgG	93H1	CST
PKCα (pT497)	Alexa488	IgG1	K14-984	BD
Phosphotyrosine	Alexa647	IgG2b	PY20	BL
SHP2 (pY542)	PE	IgG1	L99-921	BD
Control Abs	**Label**	**Subclass**	**Clone**	**Supplier**
IgG1 control	FITC or PE	IgG1	MOPC-21	BD
IgG2a control	PE	IgG2a	G155-178	BD
IgG2b control	PE	IgG2b	27-35	BD
IgG1 control	APC	IgG1	MOPC-21	BL

Supplier Abbreviations: BD = BD Biosciences (San Jose, CA, USA); BL = BioLegend (San Diego, CA, USA); CST = Cell Signaling Technology (Beverly, MA, USA)

percentile)] / Median. This calculation is not affected by the number of cell events.

Statistical analysis

Comparison between each data set was performed by one-way or two-way analysis of variance with a *post hoc* Bonferroni test. A two group comparison was performed with a paired *t*-test. Correlation was calculated with the Pearson R test. Data analysis was performed using Prism Software (v5.03, GraphPad Software, San Diego, CA, USA). *P* values less than 0.05 were considered significant. A bubble chart graph was plotted by Graph-R (v2.19, Vector, http://www.vector.co.jp/soft/winnt/business/se136959.html).

Results

Theoretical section

Theoretical recognition of biological systems

Statuses of components (cells, signal transducers, or metabolites) in biological systems continuously fluctuate and are gradually drawn to attractants. The fluctuation and attraction are repeated, and the itinerant history of the attracted components decides the fate of biological responses[24]. This premise allows us to speculate as follows: When stimulation induces change of status, the representative change of status, i.e., observable action, can be discovered in the upper layer (Fig. 1A). In the lower layer, fluctuation and contraction of status simultaneously occur as undetectable actions (Fig. 1A). Furthermore, fluctuation is required to change the status prior to attraction to the representative action. Therefore, undetectable action in the lower layer consists of fluctuation and contraction of status.

From another point of view, statuses of components in biological systems are expressed by multi-parametric coordinates (Fig. 1B). For example, the status of a single cell is expressed as a dot (shown as a blue bubble in Fig. 1B) on the coordinate, so that the cluster of these cells is presented as a cluster of dots, which is similar to results obtained by flow cytometry analysis. As described above (Fig. 1A), the status of the cluster is changed to contraction from fluctuation by stimulation. Therefore, contraction of the dots indicates attraction, and divergence of the dots shows fluctuation. The contracted status is transited (recognized as a representative response) to the upper layer on another multi-parametric coordinate. Kinetic projection indicates the process of attraction to contractive status, such as time course, calcium influx, phosphorylation of signal transducers, etc. Thus, the changing status of cell clusters will also show the contraction or fluctuation on a multi-parametric coordinate.

Utilization of CV and MFI to examine biological responses

The status of components in biological systems is expressed by coordinates, and the status of clusters is projected on a planar view of simple parameters as shown in Fig. 1B. MFI is well used for the analysis using flow cytometry. However, MFI is not suitable for detection of contraction or fluctuation of biological responses, since MFI is value of average of the events. In this study, we propose to use CV to analyze contraction or fluctuation of the events.

To understand the utilization of CV and MFI in biological responses, a schema of a single parametric phase of biological responses is shown in Fig. 2. The blue bubbles indicate single cells, and the red arrows show kinetic direction of cells after stimulation.

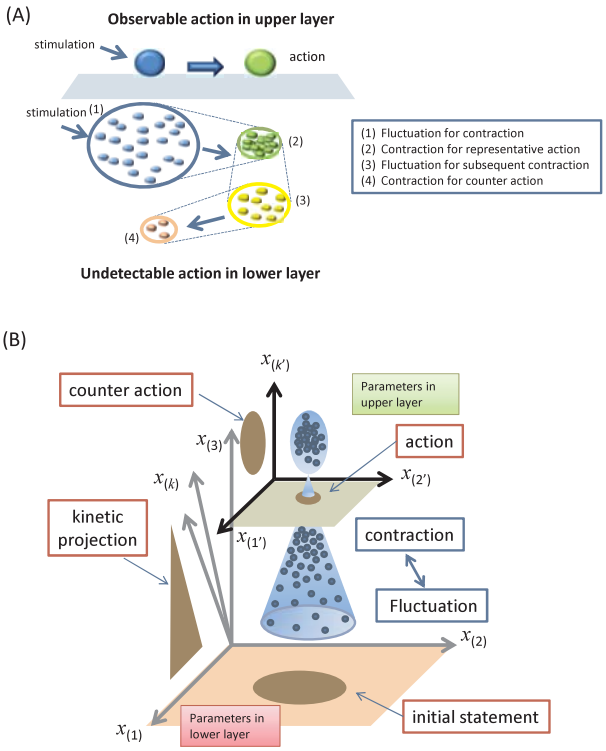

Figure 1. Relationship between hierarchy of phenomena and transition of fluctuation to contraction.
(A) Image schema of itinerant history of biological responses. The bubbles indicate components (cells, signal transducers, or metabolites), and the circles indicate clusters of these components in a biological system. The colors indicate change of status. The size of the circle represents contraction and fluctuation.
(B) Representation of biological response on multi-parametric coordinates. The small blue bubbles are the components in the biological system. The light blue areas are clusters of bubbles. The gray geometries show simple parameters on multi-parametric coordinates.

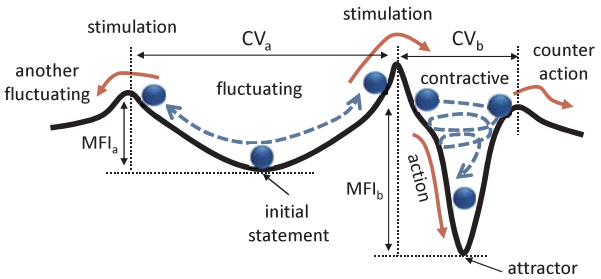

Figure 2. A schema of a single parametric phase of biological responses using coefficient variation (CV) and mean of fluorescence intensity (MFI).
Utilization of CV and MFI from flow cytometry analysis for schema of biological responses on a single parametric phase. Blue bubbles indicate single cells. Red arrows indicate cell movement after stimulation. Dotted blue arrows indicate stochastic cell position or cell movement before and after stimulation. The range of stochastic cell position is applied to CV. The energy (or speed of cell movement) to overcome initial attraction or another fluctuation is related to MFI.

Dotted blue arrows indicate stochastic cell position or kinetic energy of cells before and after stimulation. The range of stochastic cell positions is applied to CV. Kinetic energy, i.e., the speed of fluctuating cells, to overcome the attractor (or another fluctuation) is related to MFI. Before initiation of attraction, both MFI and CV increase, and when cells enter the attraction (action), CV decreases and MFI increases.

Experimental section

Verification of MFI and CV during stimulation

To verify this hypothesis, Jurkat cells were stimulated with IFN- α or IL-21, and then the phosphorylated signal transducers were stained with each specific antibody. Finally, these cells were measured by flow cytometry. The fluctuations of cell clusters are detected as the CV of cell histograms, and the kinetic energy is considered as MFI. Representative analysis of flow cytometry is presented in Fig. 3. In this study, CV was calculated as robust CV, which is not affected by cell count (total event numbers). MFI was calculated as the average of the sums of fluorescence of a single cell. Although the MFI results are already known results, the CV results are completely new data.

CV, i.e., cell fluctuation, should be increased during stimulation, and the decrease of CV should be observed after the initiation of attraction, i.e., action (Fig. 2). The time course (time kinetics) observations help to understand the relationship between CV and kinetics of signal transducers (Fig. 4). As shown in the %change of MFI (Fig. 4, left-hand side panels), which indicates kinetics of signal activation, IFN- α temporally induced the phosphorylation of STAT1 (pSTAT1), and IL-21 also induced the temporal phosphorylation of STAT3 (pSTAT3) from 10 to 30 min following treatment. After 30 min, the phosphorylation of STAT1 and STAT3 decreased. On the other hand, %change of MFI in pERK1/2 and pSTAT5 were not significantly changed by the stimulations. The change patterns (increase and

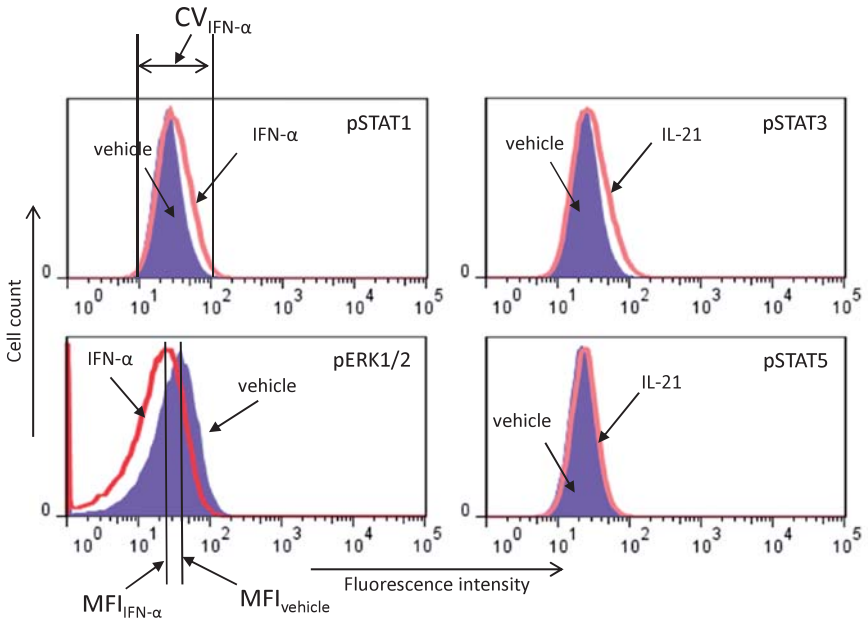

Figure 3. Representative analysis of coefficient variation (CV) and mean of fluorescence intensity (MFI) using histograms of phosphorylated signal transducers. Jurkat cells were stimulated with vehicle, IFN-α (100 U/mL), or IL-21 (1 nM) for 10 min. The representative overlay histograms of phosphorylated signal transducers, such as pSTAT1, pSTAT3, pSTAT5, and pERK1/2, are shown (blue shading = vehicle; red line = IFN-α or IL-21 stimulation). Representative analysis of CV is shown in the upper left histogram panel. The CV was calculated as described in Materials and Methods.

decrease) of CV of each signal transducer were similar to %change of MFI (Fig. 4, right-hand side panels). Therefore, specific activations of signal transducers were observed with both MFI and CV. Interestingly, %change of MFI on pSTAT1 at 90 min was significantly augmented by stimulation with IFN-α compared with that of the vehicle at 90 min. However, CV was decreased (contractive) at 90 min. This contraction of CV and increase of MFI at 90 min were considered as the time of entrance into attraction. Thus, these results suggested that the change of MFI and CV was suitable for testing our hypothesis.

To validate the relationship between the change of CV and dose of stimulants, the cells were stimulated with various doses of IFN-α (Fig. 5A and 5B) or IL-21 (Fig. 5C and 5D). There was no discrepancy pattern between %change of MFI (Fig. 5A and 5C) and CV (Fig. 5B and 5D) at 10 and 30 min stimulations (before contraction). These results suggested that fluctuation (increase of CV) was not only augmented by low dose stimulations, but also by higher dose stimulations.

Finally, correlation of CV to %change of MFI (change ratio from the initial MFI at 0 min) at 10 and 30 min stimulations (Fig. 6A and 6B) and level of MFI (Fig. 6C and 6D) were analyzed. Although %change of MFI was significantly correlated with CV, the levels of MFI were not correlated with CV. These results suggested that the initial states of MFI at 0 min were not correlated with CV at 0 min; furthermore, the attracted state of MFI at 90 min was also not correlated with CV at 90 min. These discrepancies at initiation and attraction points strongly suggest that fluctuating CV and contractive CV changed independently of MFI during stimulation. These observations also indicated that the change of MFI and CV was suitable for testing our hypothesis.

Pattern of CV change during decrease of MFI

The ERK1/2 pathway is observed as oscillation and fluctuation. The pathway is activated in discrete, asynchronous pulses with frequency and duration determined by extracellular concentrations of stimulant[9]. Furthermore, the frequency of pulse

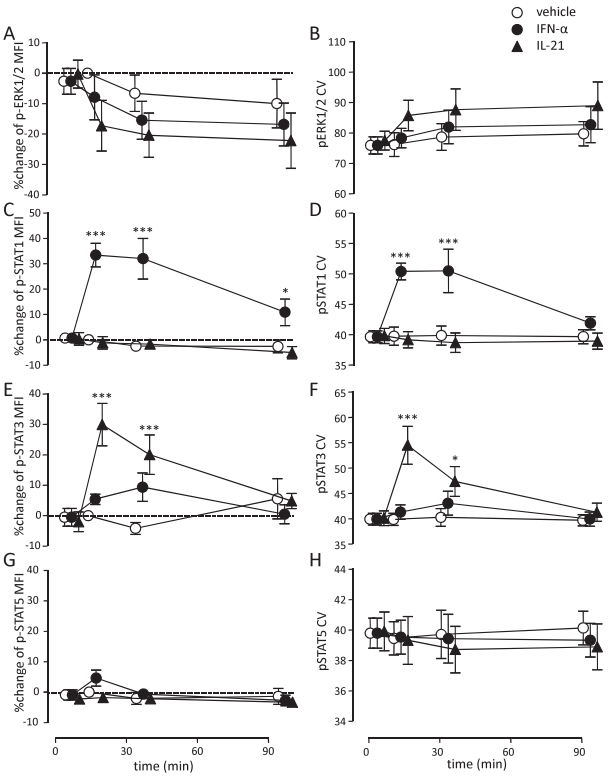

Figure 4. Change of mean of fluorescence intensity (MFI) and coefficient variation (CV) after the addition of IFN-α or IL-21.
Jurkat cells were incubated with vehicle (open circle), IFN-α (closed circle, 100 U/mL), or IL-21 (closed triangle, 1 nM) for 0, 10, 30, and 90 min. After the incubation, the cells were fixed and analyzed by flow cytometry. The cells were stained with each antibody to detect pERK1/2 (A and B), pSTAT1 (C and D), pSTAT3 (E and F), and pSTAT5 (G and H). Left-hand side panels (A, C, E, and G) show %change of MFI, calculated as follows: %change of MFI = 100 × [(MFI of cytokine at incubation time) − (MFI of vehicle at 10 min incubation)] / (MFI of vehicle at 10 min incubation). Right-hand side panels (B, D, E, and G) indicate CV. Data are mean ± SE, n = 4. The comparisons between 0 min and each time point were performed using two-way ANOVA with Bonferroni's post hoc test. Asterisks denote significant differences vs. vehicle (*, $P < 0.05$; **, $P < 0.01$; ***, $P < 0.001$).

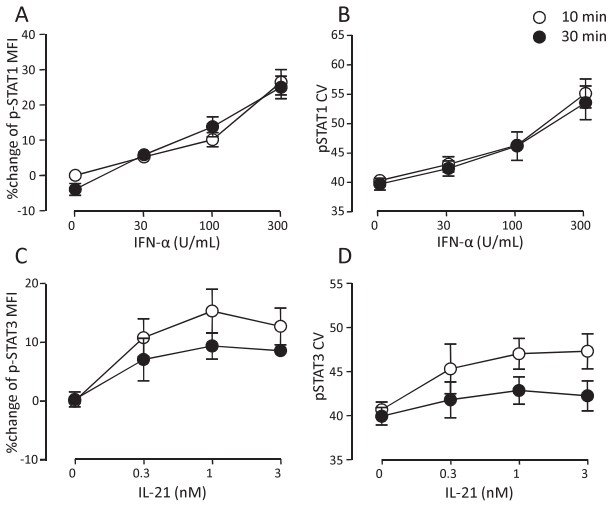

Figure 5. Effect of cytokine doses on %change of MFI and CV.
Jurkat cells were activated by various doses of cytokines for 10 min (open circle) or 30 min (closed circle). The doses of IFN-α (A and B) were 0, 33, 100, and 300 U/mL, and the doses of IL-21 (C and D) were 0.33, 1, and 3 nM. Left-hand side panels (A and C) show %change of MFI, and right-hand side panels (B and D) show CV. Data are mean ± SE, n = 4.

determines the signal characteristics[25]. In this study, we found that ERK1/2 fluctuation was induced by stimulation with IFN-α or IL-21 (Fig. 7). These stimulants significantly increased ERK1/2 (pERK1/2) CV (Fig. 7B), which accompanied the decrease of pERK1/2 MFI (Fig. 7A). In contrast to STATs CV, pERK1/2 CV, as shown in Fig. 7C, was inversely correlated with pERK1/2 MFI at all time point. Therefore, the stimulation might reduce activating frequency and result in an increase of CV.

To clarify the inverse correlation between pERK1/2 MFI and CV, we examined another condition to reduce the ERK1/2 activation. As shown in Fig. 8A, lower temperature (4°C) significantly reduced pERK1/2 MFI compared with normal conditions (37 °C). Although not significant, an increase of pERK1/2 CV was observed. Importantly, lower temperature was not sufficient stimulation to increase CV; however, an inverse correlation between pERK1/2 MFI and CV was observed. We also examined U0126 as an inhibitor of MEK1/2, which are upstream of ERK1/2 activation (Fig. 8B). Similarly, U0126 significantly reduced pERK1/2 MFI, and an inverse correlation between pERK1/2 MFI and CV was observed. These observations indicated that reduction of the ERK1/2 activating frequency induces the increase of pERK1/2 CV. Conversely, the reduction of pERK1/2 CV suggests that the pERK1/2 pathway synchronizes the oscillation and/or increases the frequency of the activation.

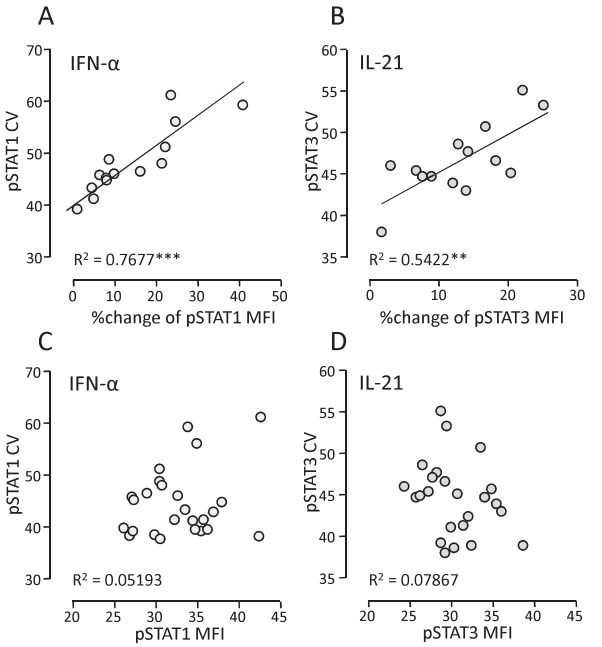

Figure 6. CV was significantly correlated to %change of MFI, but not MFI.
The CV was obtained from the results of Figure 4. Left-hand side panels show the results of IFN- α treatment, and right-hand side panels show the results of IL-21 treatment. The correlation between CV and %change of MFI (upper panels) and between CV and MFI (lower panels) are plotted with the Pearson R value. Asterisks denote significant correlation (**, $P < 0.01$; ***, $P < 0.001$).

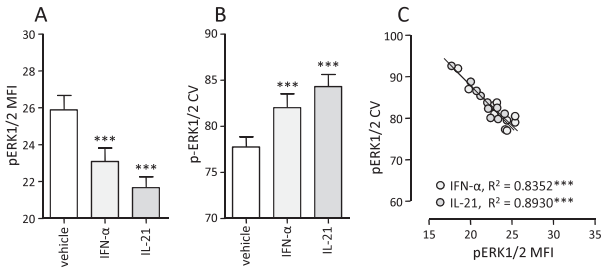

Figure 7. Down-regulation of pERK1/2 MFI by IFN- α and IL-21 and the correlation between pERK MFI and pERK CV.
Jurkat cells were stimulated with IFN-α (100 U/mL) and IL-21 (1 nM) for 10 min. MFI and CV of pERK were measured. The correlations between CV and MFI are shown in (C). Comparison of vehicle to IFN-α or IL-21 treatment was performed by one-way ANOVA with Bonferroni's *post hoc* test (***, $P < 0.001$). Data are mean ± SE, n = 10.

Multi-parametric presentation of signal pathways using bubble charts

To facilitate the visualization of fluctuation and contraction of signal transducers, we presented the

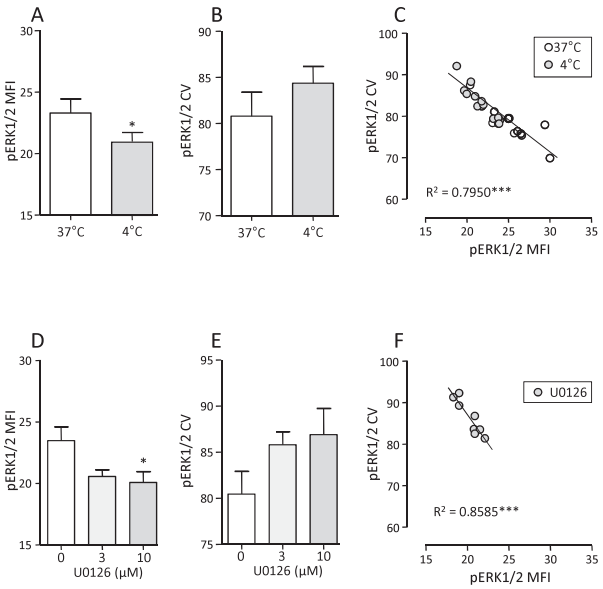

Figure 8. Down-regulation of pERK1/2 MFI and up-regulation of ERK1/2 CV by low temperature and MEK1/2 inhibitor (U0126) treatment.
Jurkat cells were incubated at 37°C or 4°C for 10 min (A, B, and C). The cells were also treated with U0126 for 10 min at 37°C (D, E, and F), and then MFI and CV of pERK were measured. Down-regulation of MFI is shown in (A) and (D), and up-regulation of CV is shown in (B) and (E). The correlations between CV and MFI are shown in (C) and (F). Statistical analysis was calculated with a paired *t*-test (A and B) and one-way ANOVA with Bonferroni's *post hoc* test (D and E) (*, $P < 0.05$; ***, $P < 0.001$). Data are mean ± SE, n = 4.

IFN-α - and IL-21-induced signaling kinetics, fluctuation of ERK1/2, and specific reactions of STATs on two-dimensional bubble charts. As shown in Fig. 9, each bubble is one sample of cell clusters. The color of the bubble indicates the time course kinetics, and the bubble diameter represents pERK1/2 CV. The x-axis and y-axis on each panel represent pSTAT1, 3, or 5. As indicated by arrows, the specific reactions to each stimulant are observed through the transition from fluctuation (blue bubbles to red bubbles) to contraction (yellow bubbles to green bubbles). The increase of pERK fluctuation by stimulation is detected by the comparison between blue bubble size and green bubble size. For example, when the cells were stimulated with IL-21, red and yellow bubble density decreased (10 min and 30 min) at higher pSTAT3 CV values, and green bubble density (90 min) increased at lower pSTAT3 CV values.

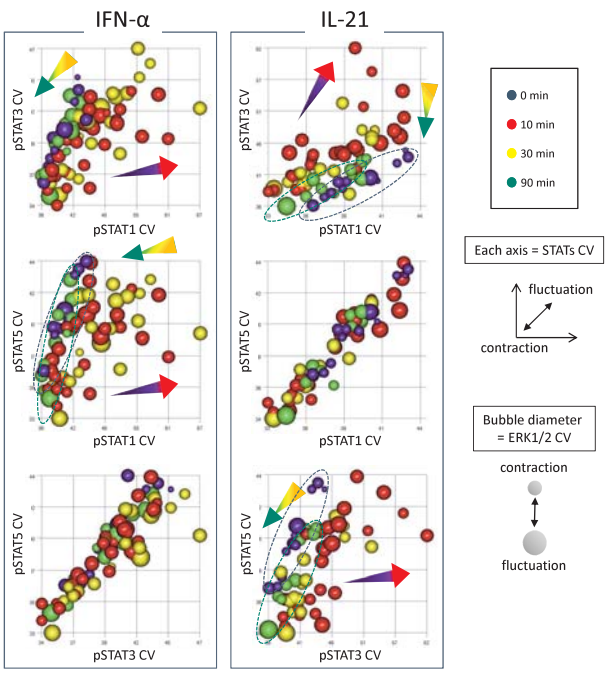

Figure 9. Bubble chart analysis of time course and pERK1/2 fluctuation plotted on pSTATs axes.
Bubble chart graphs were drawn with Graph-R software. Bubble color indicates time course: blue = 0 min; red = 10 min; yellow = 30 min; green = 90 min. Bubble diameter represents the value of pERK1/2 CV. Combinations of x-axes and y-axes are as follows: upper panels = pSTAT1 CV (x) and pSTAT3 CV (y); middle panels = pSTAT1 CV (x) and pSTAT5 CV (y); lower panels = pSTAT3 CV (x) and pSTAT5 CV (y). The left-hand side panels show results of stimulation with IFN-α, and the right-hand side panels show results of stimulation with IL-21.

Subsequently, pSTAT1 CV also transitioned from fluctuation to contraction. The size of green bubbles (90 min) was larger than that of blue bubbles (0 min), and each bubble size was larger at lower pSTATs CV values compared to that at higher pSTATs CV values with IL-21 treatment. The positions of the blue bubbles (0 min) indicated by the blue dashed ellipses were changed to the reduced positions of the green bubbles (90 min) shown by the green dashed ellipses. The changing of bubble position on the CV-axes with bubble size related to CV of another signal transducer may help visualization of contractive and fluctuating signals.

Table 2. Categorization of signal transducer status and function

Category	MFI	Status and Function
Contractive signals (CV↓)		
Attractive	Increase↑	Attract to representative action (This signal relates to observable action.)
Negative arbiter	Decrease↓	Augment the attraction (Before stimulation, this signal is competitive with attractive signals.)
Fluctuating signals (CV↑)		
Subsequent	Increase↑	Related to next or alternative attraction (This signal suggests existence of other cell subsets or subsequent action.)
Counter	Decrease↓	Augment the attraction by increasing fluctuation (This signal contributes to maintaining homeostasis after the stimulation.)
Passive signals (CV→)		
Passive	Unchanged or unclear →	None contributed, bystander (This signal will be influenced by perturbation.)

Categorization of signal transducers by combination of MFI and CV

In a heterogeneous cell population, the determination of the activated signal transduction pathways is difficult, since the initial status of each cell is not same. However, heterogeneity is universal. In this study, lymphocytes, which were not divided into B cells or T cells, were used for analysis of signal pathways with CV and MFI. In spite of that, the signal pathways in lymphocytes could be categorized by a combination of MFI and CV (Table 2 and Fig. 10). We categorized signals into three classes (contractive signals, fluctuating signals, and passive signals) by CV because the contraction is considered related to observable action in the upper layer (Fig. 1). The contractive signals were further separated into two categories, attractive signals and negative arbiter signals, based on increase and decrease of MFI, respectively. The fluctuating signals were also separated into two categories, subsequent signals and counter signals, based on increase and decrease of MFI, respectively. The third category was passive signals, which do not induce a clear change in both CV and MFI. The categorization was consistent with the previous observations of signal transduction activated by IL-21, and could explain the function of IL-21 on lymphocytes[14), 26), 27)], i.e., IL-21 mainly activates STAT3 in various lymphocytes, and alternatively activated STAT1 and STAT3 depend on lymphocyte type. These results suggested that it is possible to analyze the signals not only under ideal

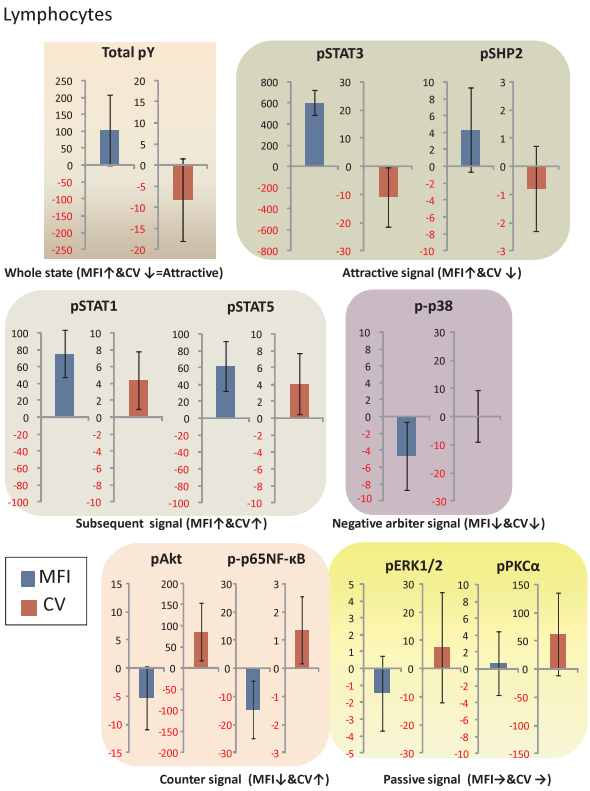

Figure 10. Categorization of signal transducers in lymphocytes by combination of MFI and CV.
Whole blood was stimulated with IL-21 (1 nM) for 10 min. For the determination of basal status, whole blood was added to the vehicle diluents of IL-21 (PBS) and incubated for 10 min. These bloods were immediately fixed after the 10 min, and then phosphorylation of various signal transducers was measured as described in Materials and Methods. Lymphocytes were detected as myeloid linage marker (CD16 or CD11b) negative cells and SSC^{low} populations. The kinetics of increase (plus) or decrease (minus) were calculated as follows: MFI kinetics (blue column) = (the value of MFI at 10 min treatment with IL-21) − (the value of MFI at 10 min treatment with PBS) or CV kinetics (red column) = (the value of CV at 10 min treatment with IL-21) − (the value of CV at 10 min treatment with PBS). The categorization of the signals was based on the data shown in Table 2. Total pY indicates total phosphotyrosine. Similarly, the name of each signal transducer is indicated above the respective panels. Data are mean ± SD (n = 3).

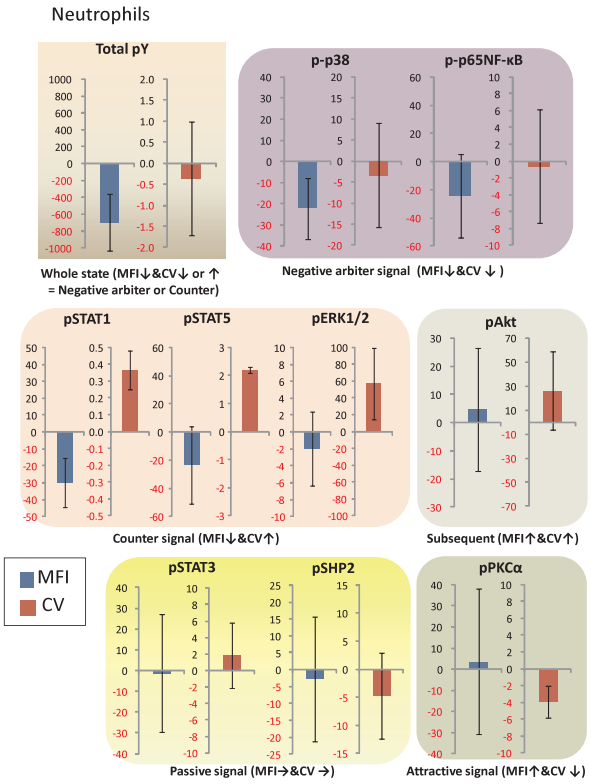

Figure 11. Categorization of signal transducers in neutrophils by combination of MFI and CV.
Whole blood was stimulated with IL-21 (1 nM) for 10 min. For the determination of basal status, whole blood was added to the vehicle diluents of IL-21 (PBS) and incubated for 10 min. These bloods were immediately fixed after the 10 min, and then phosphorylation of various signal transducers was measured as described in Materials and Methods. Neutrophils were gated by CD16 (or CD11b) positive and SSC^{high} populations. The kinetics of increase (plus) or decrease (minus) were calculated as follows: MFI kinetics (blue column) = (the value of MFI at 10 min treatment with IL-21) − (the value of MFI at 10 min treatment with PBS) or CV kinetics (red column) = (the value of CV at 10 min treatment with IL-21) − (the value of CV at 10 min treatment with PBS). The categorization of the signals was based on the data shown in Table 2. Total pY indicates total phosphotyrosine. Similarly, the name of each signal transducer is indicated above the respective panels. Data are mean ± SD (n = 3).

conditions using the cell line but also with any gated cell population using heterogeneous peripheral blood cells.

When neutrophils were stimulated with IL-21, the phosphorylation of STAT3 (MFI) was decreased, and the phosphorylation of other signal transducers was not induced[23]. These responses are commonly considered to be due to non-responsive cells; however, MFI of p38 MAPK and STAT1 were decreased, and CV of STAT1, STAT5, and ERK1/2 were increased (Fig. 11). These results suggested that neutrophils were responsive to IL-21, which induced negative arbiter signals and counter signals. Therefore, the categorization provides an opportunity for novel

recognition of phenomena, functions, cell subsets, and molecular interactions.

Discussion

Predicting the reaction cascade of enzymes in signal transduction pathways, which are hyper-complex systems, is extremely difficult because the pathways are amplified and controlled by various spatio-temporal mechanisms, such as cross-over interaction, feedback, or protein modifications, under heterogeneous conditions.

In this study, we demonstrated that the CV of signal transducers indicated kinetics of signal pathways in the Jurkat cell line. The decrease of CV suggests a contraction of signal status, and the increase of CV indicates a fluctuation of signal status. In heterogeneous conditions (whole blood), the CV decrease was closely related with observable action. Furthermore, the combination of MFI and CV provides a novel categorization of signal pathways as follows: contractive signals (consisting of attractive signals and negative arbiter signals), fluctuating signals (consisting of subsequent signals and counter signals), and passive signals.

Neutrophils are not a simple population. Five subsets were detected in a mouse neutrophil population by a 38-antibody panel using mass cytometry[28]. However, there are limits in detection of minute differences among surface antigens because neutrophil surface antigens vary with methods of neutrophil separation or the process of neutrophil maturation[23), 29)]. Instead of high-dimensional surface analysis data, the dispersion information is one of the markers for functional cell clusters in heterogeneous cells[29]. These previous observations indicate that the categorization is useful to characterize signal pathways in these heterogeneous cell clusters.

Many reports show efficacy of IL-21 for cancer treatment[30)−33)]. Recently, combined IL-21-primed polyclonal CTL plus CTLA4 blockade controlled refractory metastatic melanoma[34]. The combination of IL-21 with IFN-α boosts STAT3 activation, cytotoxicity, and experimental tumor therapy[15]. It is expected that the combined treatment of cytokines and immune checkpoint inhibitors will become more common. The categorization of signals may be more useful for prediction of combined stimulations, such as drug or cytokine combinations, on heterogeneous blood samples.

We observed the counter signals belonging to the fluctuating signals. Observable action implies robust attraction among other signals. We speculate that the counter signals may maintain dynamic equilibrium as follows: Negative arbiter signals (a_0) and attractive signals (a_1) are important for action, but are risk factors for homeostasis. The subsequent signals (a_2) are candidates for the next attractions; thus, the number of attraction signals ($a = a_0 + a_1 + a_2$) should be lower than the number of counter signals (c), i.e., homeostasis is $a < c$, and prolapse of homeostasis is $a > c$. In Jurkat cells, ERK1/2 pathway is considered a counter signal during stimulation with IL-21 or low temperature. The investigation of counter signals may open a new avenue to analyze dynamic equilibrium.

In this study, we proposed novel recognition methods of signal pathways using flow cytometry. The contraction and fluctuation of cell clusters are useful to categorize the signal characteristics. We expect that this method can be applied to various molecule statuses and evolve into an effective technique to replace high-dimensional analysis.

Acknowledgements

This work was supported by Grant-in-Aid for Scientific Research No. 22590432. We would like to thank Ms. Marina Matusmoto, Mr. Yoshihiro Shigehara, Mr. Yuki Ishizawa, and Mr. Syunsuke Koyama (medical students at Yamagata University Faculty of Medicine) for valuable technical support.
We are grateful to Ms. Akemi Araki (Department of Immunology, Yamagata University Faculty of Medicine) for her helpful suggestions.

Disclosure

The authors have no disclosures.

References

1. Wada A: Seimei no bunnshi-buturi-teki haikei-kinndaiteki seimeironn no sidou-. Nihonn Butsuri-gaku gakkaishi 1996; 51: 83-90
2. Fraser ID, Germain RN: Navigating the network: signaling cross-talk in hematopoietic cells. Nat Immunol 2009; 10: 327-331
3. Androulakis IP, Kamisoglu K, Mattick JS: Topology and dynamics of signaling networks: in search of transcriptional control of the inflammatory response. Annu Rev Biomed Eng 2013; 15: 1-28
4. Xu TR, Vyshemirsky V, Gormand A, von Kriegsheim A, Girolami M, Baillie GS, Ketley D, Dunlop AJ, Milligan G, Houslay MD, Kolch W: Inferring signaling pathway topologies from multiple perturbation measurements of specific biochemical species. Sci Signal 2010; 3: ra20
5. Tobe BT, Hou J, Crain AM, Singec I, Snyder EY, Brill LM: Phosphoproteomic analysis: an emerging role in deciphering cellular signaling in human embryonic stem cells and their differentiated derivatives. Stem Cell Rev 2012; 8: 16-31
6. Santra T, Kolch W, Kholodenko BN: Integrating Bayesian variable selection with Modular Response Analysis to infer biochemical network topology. BMC Syst Biol 2013; 7: 57
7. Shalek AK, Satija R, Shuga J, Trombetta JJ, Gennert D, Lu D, Chen P, Gertner RS, Gaublomme JT, Yosef N, Schwartz S, Fowler B, Weaver S, Wang J, Wang X, Ding R, Raychowdhury R, Friedman N, Hacohen N, Park H, May AP, Regev A: Single-cell RNA-seq reveals dynamic paracrine control of cellular variation. Nature 2014; 509: 363-369
8. Levine JH, Lin Y, Elowitz MB: Functional roles of pulsing in genetic circuits. Science 2013; 342: 1193-200
9. Albeck JG, Mills GB, Brugge JS: Frequency-modulated pulses of ERK activity transmit quantitative proliferation signals. Mol Cell 2013; 49: 249-261
10. Kolch W, Halasz M, Granovskaya M: Kholodenko BN, The dynamic control of signal transduction networks in cancer cells. Nat Rev Cancer 2015; 15: 515-527
11. Villarino AV, Kanno Y, Ferdinand JR, O'Shea JJ: Mechanisms of Jak/STAT signaling in immunity and disease. J Immunol 2015; 194: 21-27
12. Petricoin EF, 3rd, Ito S, Williams BL, Audet S, Stancato LF, Gamero A, Clouse K, Grimley P, Weiss A, Beeler J, Finbloom DS, Shores EW, Abraham R, Larner AC: Antiproliferative action of interferon-alpha requires components of T-cell-receptor signalling. Nature 1997; 390: 629-632
13. Takaoka A, Mitani Y, Suemori H, Sato M, Yokochi T, Noguchi S, Tanaka N, Taniguchi T: Cross talk between interferon-gamma and -alpha/beta signaling components in caveolar membrane domains. Science 2000; 288: 2357-2360
14. Asao H, Okuyama C, Kumaki S, Ishii N, Tsuchiya S, Foster D, Sugamura K: Cutting edge: the common gamma-chain is an indispensable subunit of the IL-21 receptor complex. J Immunol 2001; 167: 1-5
15. Eriksen KW, Sondergaard H, Woetmann A, Krejsgaard T, Skak K, Geisler C, Wasik MA, Odum N: The combination of IL-21 and IFN-alpha boosts STAT3 activation, cytotoxicity and experimental tumor therapy. Mol Immunol 2009; 46: 812-820
16. Kohno M, Pouyssegur J: Targeting the ERK signaling pathway in cancer therapy. Ann Med 2006; 38: 200-211
17. Chung E, Kondo M: Role of Ras/Raf/MEK/ERK signaling in physiological hematopoiesis and leukemia development. Immunol Res 2011; 49: 248-268
18. Griffith CE, Zhang W, Wange RL: ZAP-70-dependent and -independent activation of Erk in Jurkat T cells. Differences in signaling induced by H2o2 and Cd3 cross-linking. J Biol Chem 1998; 273: 10771-10776
19. Sun Y, Liu WZ, Liu T, Feng X, Yang N, Zhou HF:, Signaling pathway of MAPK/ERK in cell proliferation, differentiation, migration, senescence and apoptosis. J Recept Signal Transduct Res 2015; 35: 600-604
20. Krutzik PO, Irish JM, Nolan GP, Perez OD: Analysis of protein phosphorylation and cellular signaling events by flow cytometry: techniques and clinical applications. Clin Immunol 2004; 110: 206-221
21. Perez OD, Nolan GP: Simultaneous measurement of multiple active kinase states using polychromatic flow cytometry. Nat Biotechnol 2002; 20: 155-162
22. Oberprieler NG, Tasken K: Analysing phosphorylation-based signalling networks by phospho flow cytometry. Cell Signal 2011; 23: 14-18
23. Takeda Y, Nara H, Araki A, Asao H: Human peripheral neutrophils express functional IL-21 receptors. Inflammation 2014; 37: 1521-1532
24. Kaneko K: Seimei toha nanika -Fukuzatukei-seimei-kagaku-he-: Tokyo Daigaku Shyuppan-Kai, 2009 [second edition]
25. Toettcher JE, Weiner OD, Lim WA: Using

optogenetics to interrogate the dynamic control of signal transmission by the Ras/Erk module. Cell 2013; 155: 1422-1434
26. Mauldin IS, Tung KS, Lorenz UM: The tyrosine phosphatase SHP-1 dampens murine Th17 development. Blood 2012; 119: 4419-4429
27. Rochman Y, Spolski R, Leonard WJ: New insights into the regulation of T cells by gamma(c) family cytokines. Nat Rev Immunol 2009; 9: 480-490
28. Becher B, Schlitzer A, Chen J, Mair F, Sumatoh HR, Teng KW, Low D, Ruedl C, Riccardi-Castagnoli P, Poidinger M, Greter M, Ginhoux F, Newell EW: High-dimensional analysis of the murine myeloid cell system. Nat Immunol 2014; 15: 1181-1189
29. Takeda Y, Kato T, Ito H, Kurota Y, Yamagishi A, Sakurai T, Araki A, Nara H, Tsuchiya N, Asao H: The pattern of GPI-80 expression is a useful marker for unusual myeloid maturation in peripheral blood. Clin Exp Immunol 2016; 186: 373-386
30. Hinrichs CS, Spolski R, Paulos CM, Gattinoni L, Kerstann KW, Palmer DC, Klebanoff CA, Rosenberg SA, Leonard WJ, Restifo NP: IL-2 and IL-21 confer opposing differentiation programs to $CD8^+$ T cells for adoptive immunotherapy. Blood 2008; 111: 5326-5333
31. Thompson JA, Curti BD, Redman BG, Bhatia S, Weber JS, Agarwala SS, Sievers EL, Hughes SD, DeVries TA: Hausman DF, Phase I study of recombinant interleukin-21 in patients with metastatic melanoma and renal cell carcinoma. J Clin Oncol 2008; 26: 2034-2039
32. Davis ID, Brady B, Kefford RF, Millward M, Cebon J, Skrumsager BK, Mouritzen U, Hansen LT, Skak K, Lundsgaard D, Frederiksen KS, Kristjansen PE, McArthur G: Clinical and biological efficacy of recombinant human interleukin-21 in patients with stage IV malignant melanoma without prior treatment: a phase IIa trial. Clin Cancer Res 2009; 15: 2123-2129
33. Stolfi C, Pallone F, Macdonald TT, Monteleone G: Interleukin-21 in cancer immunotherapy: Friend or foe? Oncoimmunology 2012; 1: 351-354
34. Chapuis AG, Lee SM, Thompson JA, Roberts IM, Margolin KA, Bhatia S, Sloan HL, Lai I, Wagener F, Shibuya K, Cao J, Wolchok JD, Greenberg PD, Yee C: Combined IL-21-primed polyclonal CTL plus CTLA4 blockade controls refractory metastatic melanoma in a patient. J Exp Med 2016; 213: 1133-1139